articles

molecular pharmaceutics

Coadministration of Paclitaxel and Curcumin in Nanoemulsion Formulations To Overcome Multidrug Resistance in Tumor Cells

Srinivas Ganta and Mansoor Amiji*

Department of Pharmaceutical Sciences, School of Pharmacy, Northeastern University, 110 Mugar Life Sciences Building, Boston, Massachusetts 02115

Received November 23, 2008; Revised Manuscript Received January 24, 2009; Accepted March 11, 2009

Abstract: Development of multidrug resistance (MDR) against a variety of conventional and novel chemotherapeutic agents is a significant challenge in effective cancer therapy. Over the last several years, we have focused on a multimodal therapeutic strategy to overcome tumor MDR by enhancing the delivery efficiency to the tumor mass and lowering the apoptotic threshold by modulation of the intracellular signaling mechanisms. In this study, we have examined augmentation of therapeutic efficacy upon coadministration of paclitaxel (PTX) and curcumin (CUR), an inhibitor of nuclear factor kappa B (NFκB) as well as a potent down-regulator of ABC transporters, in wild-type SKOV3 and drug resistant SKOV3$_{TR}$ human ovarian adenocarcinoma cells. PTX and CUR were encapsulated in flaxseed oil containing nanoemulsion formulations. The results showed that the encapsulated drugs were effectively delivered intracellular in both SKOV3 and SKOV3$_{TR}$ cells. CUR administration was shown to inhibit NFκB activity and down regulate P-glycoprotein expression in resistant cells. Combination PTX and CUR therapy, especially when administered in the nanoemulsion formulations, was very effective in enhancing the cytotoxicity in wild-type and resistant cells by promoting the apoptotic response. Overall, this cotherapy strategy has significant promise in the clinical management of refractory diseases, especially in ovarian cancer.

Keywords: Multidrug resistance; paclitaxel; curcumin; nanoemulsions; combination therapy; SKOV3 ovarian adenocarcinoma cells

1. Introduction

Development of multidrug resistance (MDR) is one of the most challenging aspects of cancer chemotherapy, as resistance develops with both conventional cytotoxic agents and the recently developed targeted biological therapies.[1] In ovarian cancer, for instance, more than 70% of initially diagnosed patients are resistant to taxane therapy, and eventually all of them will be resistant upon relapse. Although clinical resistance is often manifested as refractory disease to standard chemotherapeutic regimens, there are several pathways by which tumor cells develop resistance due to microenvironment selection pressures. The most frequently occurring causes of MDR include the overexpression of ATP-binding cassette (ABC) super family of transporters, which are trans-membrane proteins that acts as a drug-efflux pump by actively removing drugs from the cells and producing intracellular drug levels below the effective concentrations necessary for cytotoxicity.[2] P-glycoprotein (P-gp), breast cancer resistance protein (ABCG2), and multidrug resistance associated protein (MRP-1) are the major transporter proteins belonging to the ABC super family that have been linked with MDR.[1] P-gp is encoded by the *MDR-1* gene

* Corresponding author. Mailing address: Northeastern University, Pharmaceutical Sciences Department, 110 Mugar Life Sciences Building, 360 Huntington Ave., Boston, MA 02115. Tel: 617-373-3137. Fax: 617-373-8886. E-mail: m.amiji@neu.edu.

(1) Szakacs, G.; Paterson, J. K.; Ludwig, J. A.; Booth-Genthe, C.; Gottesman, M. M. Targeting multidrug resistance in cancer. *Nat. Rev. Drug Discovery* **2006**, *5* (3), 219–234.

(2) Ejendal, K. F. K.; Hrycyna, C. A. Multidrug resistance and cancer: the role of the human ABC transporter ABCG2. *Curr. Protein Pept. Sci.* **2002**, *3*, 503–511.

10.1021/mp800240j CCC: $40.75
Published on Web 03/11/2009

and has been shown to overexpress with the development of MDR in tumor biopsy samples.[3] P-gp expression has been directly implicated in resistance to a broad spectrum of anticancer agents such as taxanes, anthracyclines and the vinca alkaloids.[4] Other causes of MDR include overexpression of MRP-1, changes in topoisomerase II (Topo IIα) activity, and modification in glutathione *S*-transferase activity (GST).[2,5−7]

Over the last several years, we have suggested that a rational approach to overcome MDR in clinical settings requires a multipronged strategy that combines enhancement in systemic drug delivery efficiency along with alterations in the cellular phenotype that lead to more effective cell-kill response.[8−12] Using poly(ethylene oxide)-modified poly-(epsilon-caprolactone) (PEO-PCL) nanoparticles encapsulating paclitaxel (PTX) and C6-ceramide, a lipid second messenger responsible for propagation of apoptotic signaling, we have shown that the cotherapy can have significant efficacy by restoring the apoptotic signaling in tumor cells and *in vivo* in SKOV3 human ovarian adenocarcinoma xenograft model established in female *nu/nu* mice.[11] Long-circulating PEO-PCL nanoparticles can enhance the delivery efficiency of hydrophobic molecules, such as PTX and ceramide, by passive targeting to the tumor mass through the enhanced permeability and retention (EPR) effect. In a more recent study, we have also shown that tamoxifen, an inhibitor of the ceramide metabolizing enzyme glucosylceramide synthase, which is overexpressed in MDR cells, can also augment the therapeutic efficacy of PTX *in vitro* and *in vivo* in the SKOV3 ovarian cancer model.[10]

In addition to intracellular ceramide modulation, either by exogenous delivery or inhibition of cellular metabolism, other strategies that can augment therapeutic efficacy of anticancer agents, especially by downregulating P-gp and MRP-1 expression as well as enhancing cellular apoptotic response, can be significantly beneficial in overcoming MDR. Curcumin (CUR), a naturally occurring polyphenol extracted from the rhizome *Curcuma longa*, has a long history of use as an Asian spice as well as in traditional therapies. Exciting recent studies, especially from Aggarwal's group at the University of Texas M. D. Anderson Cancer Center in Houston, have shown that CUR has a pleiotropic therapeutic effect in cancer.[13,14] The anticancer properties of CUR have been primarily attributed by its activity to block the transcriptional factor nuclear factor kappa B (NFκB), which is a master regulator of inflammation, cell proliferation, apoptosis, and resistance in cells.[15] NFκB regulates the expression of genes involved in suppression of apoptotic response and is responsible for tumor cell survival.[13] Additionally, CUR is also known to downregulate the intracellular levels of three major ABC drug transporters, P-gp, MRP-1 and ABCG2, that are important in MDR.[16,17] This pleiotropic effect of CUR is especially advantageous when administered with a delivery system that enhances bioavailability at the tumor mass and promote intracellular availability of the combination drugs upon systemic administration.

Nanoemulsions are heterogeneous mixtures of oil in water, where the oil droplets are confined to nanometer size (typically less than 200 nm). Using oils rich in omega-3 and omega-6 polyunsaturated fatty acids (PUFA), we have

(3) Molinari, A.; Calcabrini, A.; Meschini, S.; Stringaro, A.; Crateri, P.; Toccacieli, L.; Marra, M.; Colone, M.; Cianfriglia, M.; Arancia, G. Subcellular detection and localization of the drug transporter P-glycoprotein in cultured tumor cells. *Curr. Protein Pept. Sci.* **2002**, *3*, 653–670.

(4) Bellamy, W. T.; Dalton, W. S. Multidrug resistance in the laboratory and clinic. *Adv. Clin. Chem.* **1994**, *31*, 1–61.

(5) Krishnamachary, N.; Center, M. S. The MRP gene associated with a non-P-glycoprotein multidrug resistance encodes a 190-kDa membrane bound glycoprotein. *Cancer Res.* **1993**, *53* (16), 3658–3661.

(6) Deffie, A. M.; Batra, J. K.; Goldenberg, G. J. Direct correlation between DNA topoisomerase II activity and cytotoxicity in adriamycin-sensitive and -resistant P388 leukemia cell lines. *Cancer Res.* **1989**, *49* (1), 58–62.

(7) Morrow, C. S.; Cowan, K. H. Glutathione S-transferases and drug resistance. *Cancer Cells* **1990**, *2* (1), 15–22.

(8) van Vlerken, L. E.; Duan, Z.; Seiden, M. V.; Amiji, M. M. Modulation of Intracellular Ceramide Using Polymeric Nanoparticles to Overcome Multidrug Resistance in Cancer. *Cancer Res.* **2007**, *67* (10), 4843–4850.

(9) van Vlerken, L. E.; Duan, Z.; Little, S. R.; Seiden, M. V.; Amiji, M. M. Biodistribution and Pharmacokinetic Analysis of Paclitaxel and Ceramide Administered in Multifunctional Polymer-Blend Nanoparticles in Drug Resistant Breast Cancer Model. *Mol. Pharmaceutics* **2008**, *5* (4), 516–526.

(10) Devalapally, H.; Duan, Z.; Seiden, M. V.; Amiji, M. M. Modulation of Drug Resistance in Ovarian Adenocarcinoma by Enhancing Intracellular Ceramide Using Tamoxifen-Loaded Biodegradable Polymeric Nanoparticles. *Clin. Cancer Res.* **2008**, *14* (10), 3193–3203.

(11) Devalapally, H.; Duan, Z.; Seiden, M. V.; Amiji, M. M. Paclitaxel and ceramide co-administration in biodegradable polymeric nanoparticulate delivery system to overcome drug resistance in ovarian cancer. *Int. J. Cancer* **2007**, *121* (8), 1830–1838.

(12) Jabr-Milane, L. S.; van Vlerken, L. E.; Yadav, S.; Amiji, M. M. Multi-functional nanocarriers to overcome tumor drug resistance. *Cancer Treat. Rev.* **2008**, *34*, 592–602.

(13) Aggarwal, B. B. Nuclear factor-kB: the enemy within. *Cancer Cell* **2004**, *6*, 203–208.

(14) Garg, A.; Aggarwal, B. B. Nuclear transcription factor-kappa B as a target for cancer drug development. *Leukemia* **2002**, *16*, 1053–1068.

(15) Aggarwal, B. B.; Shishodia, S.; Takada, Y.; Banerjee, S.; Newman, R. A.; Bueso-Ramos, C. E.; Price, J. E. Curcumin suppresses the paclitaxel-induced nuclear factor-{kappa}B pathway in breast cancer cells and inhibits lung metastasis of human breast cancer in nude mice. *Clin. Cancer Res.* **2005**, *11* (20), 7490–7498.

(16) Limtrakul, P.; Chearwae, W.; Shukla, S.; Phisalphong, C.; Ambudkar, S. V. Modulation of function of three ABC drug transporters, P-glycoprotein (ABCB1), mitoxantrone resistance protein (ABCG2) and multidrug resistance protein 1 (ABCC1) by tetrahydrocurcumin, a major metabolite of curcumin. *Mol. Cell. Biochem.* **2007**, *296* (1), 85–95.

(17) Chearwae, W.; Wu, C. P.; Chu, H. Y.; Lee, T. R.; Ambudkar, S. V.; Limtrakul, P. Curcuminoids purified from turmeric powder modulate the function of human multidrug resistance protein 1 (ABCC1). *Cancer Chemother. Pharmacol.* **2006**, *57* (3), 376–388.

developed a number of different nanoemulsion formulations for oral and systemic administration.[18−21] The advantages of nanoemulsions include an opportunity to solubilize hydrophobic compounds, such as PTX and CUR, in the oil phase, surface modification of the oil droplets with poly(ethylene glycol) (PEG) to allow for long-circulation times and passive tumor targeting and/or active targeting ligands, and use of safe edible materials [e.g., food grade oils and "generally regarded as safe" (GRAS) grade excipients] for fabrication of the delivery system. We have also engineered nanoemulsions to carry multiple payloads (e.g., PTX and ceramide) or combination of drug and image contrast enhancers (e.g., gadolinium ions for MRI).[21,22] Additionally, scale up and reproducibility of nanoemulsions are facilitated by using large scale high energy microfludic devices.[19]

In this study, we have examined the combination delivery of PTX and CUR, encapsulated in flaxseed oil containing nanoemulsions, for enhancement of efficacy in wild-type (drug sensitive) SKOV3 and drug resistant $SKOV3_{TR}$ human ovarian adenocarcinoma cells. In addition to formulation design and optimization, we have examined intracellular delivery, downregulation of P-gp and inhibition of NFκB pathway, enhancement of cell-kill efficacy, and the apoptotic response following treatment with single and combination therapy in aqueous solution and nanoemulsion formulations.

2. Materials and Methods

2.1. Materials. High omega-3 fatty acid-containing flaxseed oil was kindly provided by Jedwards International (Quincy, MA). CUR and 3-[4,5-dimethylthiazolyl]-2,5-diphenyltetrazolium bromide (MTT reagent) were purchased from the Sigma Chemicals (St. Louis, MO), while PTX was obtained from LC Laboratories (Woburn, MA). Egg phosphotidylcholine (Lipoid E80) was obtained from the Lipoid GmbH (Ludwigshafen, Germany) and 1,2-distearoyl-*sn*-glycero-3-phosphoethanolamine-*N*-[methoxy-(polyethylene glycol)-2000] (DSPE-PEG_{2000}) was purchased from Genzyme Corporation (Cambridge, MA). The hydrophobic fluorophore, 1,1′-dioctadecyl-3,3,3′,3′-tetramethylindodicarbocyanine perchlorate (DiD dye) was obtained from Invitrogen (Carlsbad, CA). Rhodamine-conjugated PTX was purchased from Natural Pharmaceuticals (Beverley, MA). Propidium iodide and YO-PRO-1 were purchased from Molecular Probes (Eugene, OR). ApoONE Homogenous Caspase-3/7 Assay Kit and the DeadEnd Colorimetric Apoptosis Detection System (TUNEL assay) were purchased from Promega (Madison, WI). SKOV3 human ovarian adenocarcinoma cells were purchased from American Type Culture Collections (Manassas, VA). Multidrug resistant $SKOV_{TR}$ cells, shown to be *MDR-1* positive, were kindly provided by Dr. Zhenfeng Duan at the Massachusetts General Hospital (Boston, MA). Anti-IκBα antibody and anti-NFκB p65 antibody were purchased from Abcam (Cambridge, MA). Anti-β-actin monoclonal antibody and horseradish peroxidase conjugated secondary antibody were obtained from Cell Signaling Tech (Danvers, MA). Anti-P-glycoprotein monoclonal antibody C219 was purchased from Calbiochem (Gibbstown, NJ). BCA proteins assay kit and chemiluminescence substrate were obtained from Thermo Scientific (Rockford, IL). All other chemicals and solvents were of reagent grade.

2.2. Preparation of Nanoemulsion Formulations. Flaxseed oil-containing nanoemulsions were prepared by coarse homogenization followed by high energy ultrasonication method as previously described.[18,21] Briefly, the aqueous phase was prepared by adding egg lecithin (120 mg) to the deionized water (4 mL), and stirred for 15 min. PTX (10 mg) in chloroform and CUR (10 mg) in ethanol were added to flaxseed oil (1 mL) taken separately in a glass vial, nitrogen was blown in the sample to evaporate the solvent and to obtain the oil phase. Following this, the aqueous phase and the oil phase were heated individually to 70−75 °C for 2−4 min. The aqueous phase was added gradually to the oil phase and homogenized for 1 min at 6,000 rpm using a Silverson homogenizer to produce the coarse oil-in-water emulsion. The coarse emulsion was then ultrasonicated at 21% amplitude and 50% duty cycle using Vibra-Cell VC 505 ultrasound instrument (Sonics and Materials, Inc., Newtown) for 10 min to obtain the nanosized oil droplets. PEG-modified nanoemulsions were prepared similarly, except DSPE-PEG_{2000} (15 mg) was included in the aqueous phase with PTX or CUR containing poly(ethylene glycol) (PEG)-modified nanoemulsions. As a control, blank nanoemulsions without the drugs were prepared in a similar manner.

2.3. Characterization of Nanoemulsions. *2.3.1. Particle Size and Zeta Potential.* The nanoemulsion formulations were characterized for particle size and size distribution using the dynamic light scattering technique with a Brookhaven Instrument's 90Plus particle size analyzer (Holtsville, NY) at a 90° fixed angle and at 25 °C temperature. The nanoemulsions for particle size analysis were diluted with deionized distilled water before analysis, and the numbered average oil droplet hydrodynamic diameter and the polydispersity index determined. For the zeta potential, nanoemul-

(18) Tiwari, S. B.; Amiji, M. M. Improved oral delivery of paclitaxel following administration in nanoemulsion formulations. *J. Nanosci. Nanotechnol.* **2006**, *6*, 3215–3221.
(19) Ganta, S.; Devalapally, H.; Baguley, B. C.; Garg, S.; Amiji, M. Microfluidic preparation of chlorambucil nanoemulsion formulations and evaluation of cytotoxicity and pro-apoptotic activity in tumor cells. *J. Biomed. Nanotechnol.* **2008**, *4*, 165–173.
(20) Vyas, T. K.; Shahiwala, A.; Amiji, M. M. Improved oral bioavailability and brain transport of Saquinavir upon administration in novel nanoemulsion formulations. *Int. J. Pharm.* **2008**, *347* (1−2), 93–101.
(21) Desai, A.; Vyas, T.; Amiji, M. Cytotoxicity and apoptosis enhancement in brain tumor cells upon coadministration of paclitaxel and ceramide in nanoemulsion formulations. *J. Pharm. Sci.* **2008**, *97* (7), 2745–2756.
(22) Tiwari, S.; Tan, Y.-M.; Amiji, M. Preparation and In Vitro Characterization of Multifunctional Nanoemulsions for Simultaneous MR Imaging and Targeted Drug Delivery. *J. Biomed. Nanotechnol.* **2006**, *2*, 217–224.

sion samples were diluted with deionized distilled water and placed in the electrophoretic cell of the Brookhaven Instrument's ZetaPALS and the average surface charge was determined.

2.3.2. Transmission Electron Microscopy (TEM). TEM analysis was used to determine the nanoemulsion morphology. For this analysis, nanoemulsions were placed on Formvar-coated copper grids (Electron Microscopy Science, Hatfield, PA) and negatively stained with 50 μL of 1% (w/v) uranyl acetate, and the staining was allowed to proceed for 10 min at room temperature. After excess liquid was drained off with a Whatman filter paper, the grid containing the nanoemulsion sample as a dry film was observed with a JEOL 100X transmission electron microscope (Peabody, MA).

2.4. Analysis of Paclitaxel and Curcumin Incorporation. A high-performance liquid chromatography (HPLC) assay was used to determine the levels of PTX and CUR incorporated in the nanoemulsion formulations. A Waters LC (model 2487, Waters Corporation, Milford) consisting of two pumps, an autosampler, and UV-detector was used for the analysis. The LC system was interfaced with the Empower software for instrument control, data acquisition, and processing. The mobile phase was made of acetonitrile and water (55:45, v/v) and was pumped through the Waters Sphersorb column (C_{18}, particle size 5 μm, 4.6 mm $\times$ 150 mm) at a 1 mL/min flow rate and PTX elution monitored at a wavelength of 230 nm. For CUR analysis, acetonitrile and 1% citric acid solution (pH 3 adjusted with 1 M sodium hydroxide solution) (50:50, v/v) at a 1 mL/min flow rate was passed through the Agilent Zorbax column (C_{18}, particle size 5 μm, 4.6 mm $\times$ 150 mm), and CUR elution monitored at 428 nm. A 10 μL aliquot was injected into the HPLC for analysis.

The PTX and CUR encapsulation efficiency in the nanoemulsion formulation was determined by an ultrafiltration method using centrifugal filter devices (molecular weight cutoff 3,000 daltons; Centricorn, Millipore, Bedford, MA). Nanoemulsion sample (1 mL) was placed in the upper donor chamber and the unit was centrifuged at 11,000 rpm for 30 min. The sample along with encapsulated drug remained in the donor chamber and aqueous phase moved into the sample recovery chamber through the filter. The concentration of the PTX and CUR in the aqueous phase was estimated using HPLC.

2.5. Stability of Nanoemulsions and the Encapsulated Drugs. The physical stability of nanoemulsion formulations was monitored over 3 months upon storage at 4 and 25 °C. During this storage period, the particle size and size distribution were determined using Brookhaven Instrument's 90Plus particle size analyzer. The chemical stability of PTX and CUR in the nanoemulsions stored at 4 and 25 °C for up to 3 months period was determined using above-described HPLC assay.

2.6. Cellular Uptake and Intracellular Availability with Nanoemulsions. *2.6.1. Cell Culture Conditions.* Human ovarian adenocarcinoma cell line, SKOV3 wild-type (drug sensitive) and $SKOV3_{TR}$ (multidrug resistant, *MDR-1* positive) were grown in RPMI medium supplemented with 10% fetal bovine serum and 1% penicillin/streptomycin. Cell cultures were maintained in a humidified 95% O_2/5% CO_2 atmosphere at 37 °C. For the subculture, cells growing as monolayer were detached from the tissue culture flasks by treatment with 0.05% trypsin/EDTA. The viability and cell count were monitored routinely using trypan blue dye exclusion method.

2.6.2. Intracellular Delivery with Nanoemulsions. Fluorescently labeled nanoemulsion samples were prepared by replacing PTX with rhodamine-conjugated PTX (0.1%) and CUR with DiD dye (0.005%), respectively, for cellular uptake and distribution studies. These fluorescent markers were added to the oil phase, and the respective nanoemulsions prepared as previously described. Cells were plated on glass coverslips in six-well microplates and incubated with 20 μL of rhodamine-paclitaxel and DiD dye containing nanoemulsions diluted with 2 mL of media per well. After 6 h of incubation, cells were washed and coverslips were fixed onto glass slides with Fluoromount-G medium. Bright-field and fluorescence microscopy images were obtained at 20$\times$ magnification on an Olympus fluorescence microscope.

2.7. Evaluation of P-gp and NFκB Activity by Western Blotting. SKOV3 and $SKOV3_{TR}$ cells growing in T-25 flasks were treated with 20 μM concentration of CUR in aqueous solution, nanoemulsion and PEG-modified nanoemulsion for 24 h. Following this treatment, the cells were lysed and the total protein was extracted and quantified by BCA proteins assay kit. Protein was separated on a 4−15% SDS−PAGE gradient gel and transferred on to nitrocellulose membrane. Nitrocellulose membrane blots were incubated with anti-P-gp monoclonal antibody C219, anti-NFkB p65 antibody, anti-IkBα antibody, or anti-β-actin monoclonal antibody overnight at 4 °C, followed by 1 h incubation at room temperature with a horseradish peroxidase-conjugated secondary antibody. To visualize the proteins of interest, the membranes were incubated for 5 min with enhanced chemiluminescence substrate and the exposed film was imaged using a Kodak Gel-logic 100 imaging system (Carestream Health, Rochester, NY).

2.8. Cytotoxicity with Single and Combination Therapy in Sensitive and Resistant Cells. The cytotoxicity studies were performed with both free drug and the nanoemulsion formulations containing graded concentrations of PTX, CUR and combination of PTX and CUR. Approximately 3,000 cells per well were seeded into 96-well plates and allowed to adhere overnight. The media was replaced with above graded concentration of drug solutions alone and in combination. Controls included all of the blank nanoemulsion formulations and vehicles that did not have any drug. RPMI growth media was used as a negative control and treatment with 0.25 mg/mL poly(ethyleneimine) (molecular weight 10 kDa), a cationic cytotoxic polymer, was used as positive control. Eight replicates were made for each test condition, and plates were incubated for 3 days. At the end, the media was replaced with 100 μL of MTT (1.0 mg/mL in RPMI)

reagent and the plates were incubated for 2 h. Viable cells reduce the tetrazolium compound into an insoluble formazan dye. The supernatant medium was carefully removed, and the formazan dye crystals were solubilized by adding 150 μL of dimethylsulfoxide. The plates were read at 570 nm using Bio-Tek Synergy HT plate reader (Winooski, VT), and the percent cell viability values were determined relative to the negative control.

PTX and CUR as single agents or in combination producing 50% inhibition of cell viability (IC_{50}) were calculated using GraphPad Prism 4. Additionally, PTX and CUR combination index (CI) was determined with the classic isobologram equation of Chou and Talalay.[23,24] $CI = a/A + b/B$, where a is the PTX IC_{50} in combination with CUR at concentration b, A is the PTX IC_{50} without CUR, and B is the CUR IC_{50} in the absence of PTX. According to this equation, when $CI < 1$, the interaction is synergistic; when $CI = 1$, the interaction is additive; and when $CI > 1$, the two agents are antagonistic.

2.9. Quantitative and Qualitative Apoptotic Activity in Sensitive and Resistant Cells. *2.9.1. Caspase-3/7 Activity.* For quantitative apoptotic analysis, SKOV3 and $SKOV3_{TR}$ cells were seeded in 96-well microplates at a density of 20,000 cells per well. Apoptosis was induced by treating the cells with PTX (10 nM for SKOV3 and 3 μM for $SKOV3_{TR}$) and CUR (10 μM) either as single agents or PTX + CUR in combination (5 nM PTX + 5 μM CUR for SKOV3 and 2 μM PTX + 5 μM CUR for $SKOV3_{TR}$), administered in aqueous solution or in nanoemulsion formulations. After 2 h of incubation, the cells were washed with RPMI to wash away any drug that did not enter the cells and cells further incubated for 24 h period. After this period, 100 μL of the Apo-ONE Caspase-3/7 substrate solution was added to each well containing 100 μL of RPMI medium. The contents of wells were mixed using a plate shaker at 300−500 rpm for 2 h at room temperature. Fluorescence of each well was measured at an excitation wavelength of 490 nm and emission wavelength of 520 nm using Bio-Tek's Synergy HT microplate reader. Caspase-3/7 activity was reported as percent activation relative to untreated control.

2.9.2. Flow Cytometric Analysis Using YO-PRO. The SKOV3 and $SKOV3_{TR}$ cells were grown in T-25 cell culture flasks with at a seeding density of 1×10^6 cells per flask. Similar to caspase-3/7 activity measurement, the cells were treated with PTX, CUR and combination of PTX and CUR for 24 h. The cells were washed in ice-cold phosphate-buffered saline (PBS, pH 7.4) and then harvested with trypsin EDTA. After centrifugation, the cell density was adjusted to 1×10^6 cells/mL in PBS. Cells that did not receive any drug treatment served as a negative control. YO-PRO-1 stock solution, 1 μL was added to each 1 mL of cell suspension. In addition, 1 μL of propidium iodide stock solution was added to the cells to identify necrotic cells. After the incubation period for 30 min on ice, stained cells were analyzed by flow cytometry using the BD Bioscience FACS caliber (San Jose, CA) instrument equipped with an argon 488 laser. The flow cytometry results were analyzed using Cell Quest Pro software.

2.9.3. TUNEL Staining. Qualitative analysis of apoptotic activity in SKOV3 and $SKOV3_{TR}$ cells following treatment of PTX and CUR solutions and nanoemulsions was also determined by terminal transferase dUTP nick end labeling (TUNEL) assay. For this study, cells growing on glass coverslips in 6-well microplates were treated with PTX, CUR and combination of PTX and CUR as described above for 48 h. Cells were then fixed with 10% formaldehyde in PBS for 25 min and permeabilized with 0.2% Triton X-100 for 5 min at room temperature. After washing with PBS, the coverslips were incubated with biotinylated nucleotide mixture with terminal deoxynucleotidyl transferase enzyme. The incorporated nucleotides were detected using diaminobenzidine and hydrogen peroxide, which resulted in the development of brown-colored stain in the apoptotic cell nuclei.

2.10. Data Analysis. Data are reported as mean ± standard deviation. Comparisons between the groups were made using Student's t test and with more than two groups, ANOVA was used to compare results. The $p < 0.05$ values were considered statistically significant. All statistical analysis was performed using SPSS, version 16.

3. Results

3.1. Nanoemulsion Formulation and Characterization. PTX and CUR containing nanoemulsion formulations were prepared using high energy ultrasonication method. We optimized the processing conditions and found that a 10 min ultrasonication (energy 21%, duty cycle 50%) resulted in a nanoemulsion with particle size less than 200 nm. A prolonged ultrasonication or increased energy did not improve this result as noted previously.[25] Flaxseed oil was used as an oil phase in the nanoemulsions which is rich in PUFA such as omega-3 and omega-6 fatty acids and solubilizes a significant amount of liphophilic anticancer drugs. Flaxseed oil contains up to 57% by weight of linolenic acid, an example of omega-3 fatty acid, and 17% by weight linoleic acid, an example of omega-6 fatty acid with 18 carbons and 2 double bonds. These omega-3 and omega-6 fatty acids have shown interesting biological properties including cancer chemopreventive effects.[26] In a series of initial experiments, the optimal composition of nanoemulsion

(23) Chou, T. C.; Motzer, R. J.; Tong, Y.; Bosl, G. J. Computerized quantitation of synergism and antagonism of taxol, topotecan, and cisplatin against human teratocarcinoma cell growth: a rational approach to clinical protocol design. *J. Natl. Cancer Inst.* **1994**, *86* (20), 1517–1524.

(24) Chou, T. C.; Talalay, P. Quantitative analysis of dose-effect relationships: the combined effects of multiple drugs or enzyme inhibitors. *Adv. Enzyme Regul.* **1984**, *22*, 27–55.

(25) Ganta, S.; Paxton, J. W.; Baguley, B. C.; Garg, S. Pharmacokinetics and pharmacodynamics of chlorambucil delivered in parenteral emulsion. *Int. J. Pharm.* **2008**, *360* (1−2), 115–121.

(26) Rose, D. P.; Connolly, J. M. Omega-3 fatty acids as cancer chemopreventive agents. *Pharmacol. Ther.* **1999**, *83*, 217–244.

Table 1. Particle Size, Surface Charge and Drug Encapsulation Efficiency Measurements of the Paclitaxel and Curcumin Containing Nanoemulsions[a]

	hydrodynamic diameter			
formulation type	mean diameter (nm)	polydispersity index	zeta potential (mV)	drug encapsulation efficiency (%)
blank nanoemulsion	133 ± 1.5	0.2	−36.74 ± 2.80	
paclitaxel nanoemulsion	139 ± 1.6	0.2	−35.37 ± 2.42	100 ± 0.0
paclitaxel PEG-modified nanoemulsion	138 ± 1.6	0.3	−39.74 ± 4.13	100 ± 0.0
curcumin nanoemulsion	132 ± 1.7	0.3	−41.88 ± 2.55	98.2 ± 0.4
curcumin PEG-modified nanoemulsion	144 ± 1.5	0.2	−44.53 ± 1.02	97.4 ± 0.3

[a] The values are shown as mean ± SD, $n = 3$.

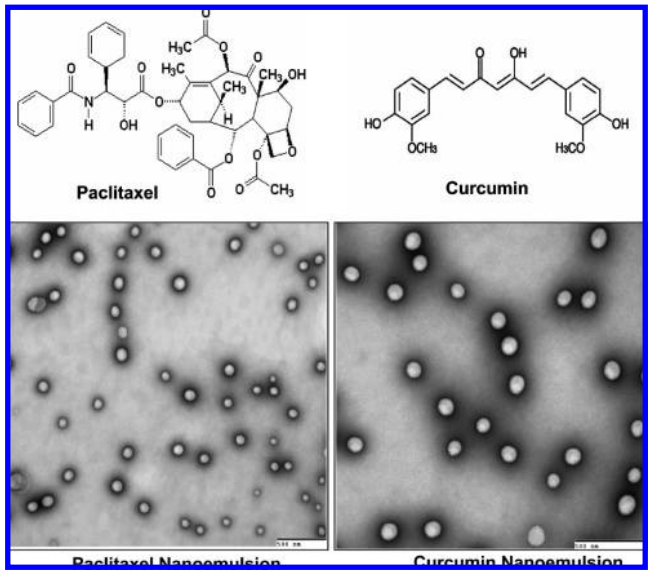

Figure 1. The chemical structures of paclitaxel and curcumin (top) and the transmission electron microscopy (TEM) images of uranyl acetate-stained paclitaxel and curcumin containing nanoemulsions (bottom). Scale bar in the TEM images is 500 nm.

formulations was evaluated with respect to oil and emulsifier concentration, particle size, and drug loading. The optimized nanoemulsion formulations consisted of PTX or CUR (0.2% w/v), flaxseed oil (20% w/v), egg phosphotidylcholine (lecithin) (1.2%, w/v) and deionized water. Additionally, PEG-modified nanoemulsions were prepared by incorporating 0.3% w/v of DSPE-PEG_{2000}.

Particle size and zeta potential (surface charge) values of nanoemulsions are summarized in Table 1. The average particle size of the blank nanoemulsion (without any drug) was 133 ± 1.5 nm. The incorporation of PTX or CUR in nanoemulsions did not significantly change the hydrodynamic particle size and size remained at approximately 133 nm. PEG-modified PTX and CUR nanoemulsions also showed approximately similar particle size. The average surface charge of the oil droplets in the nanoemulsions were in the range of −35.37 to − 44.53 mV. TEM micrographs of negatively stained nanoemulsions showed that the oil droplets were spherical and uniform in size (Figure 1).

An HPLC assay was used to determine the drug concentrations in the nanoemulsion formulations. Approximately 2.0 ± 0.02 mg/mL of PTX or 1.9 ± 0.2 mg/mL of CUR, respectively, was present in each nanoemulsion formulation. As it is seen from the Table 1, PTX encapsulation efficiency of both plain and PEG-modified nanoemulsions was 100%. On the other hand the CUR containing nanoemulsions showed about 97% encapsulation efficiency. This high drug encapsulation efficiency of nanoemulsions was attributed to the relative lipophilicity of the drugs, as these drugs retained in the oil core of the nanoemulsions. The stability results show that PTX and CUR were stable in the formulations during the 3 month storage period. Additionally, all the formulations were physically stable and no phase separation was observed. However, the slight increase in particle size was noted and the highest size reached during the storage was 183 ± 2.7 nm and still remained in the nanosize range.

3.2. Cellular Uptake of Fluorescently-Labeled Nanoemulsions. Rhodamine-labeled PTX and DID dye containing nanoemulsion formulations were incubated with SKOV3 and $SKOV3_{TR}$ cells, and their intracellular distribution was studied as shown in Figure 2. These images clearly indicate that the nanoemulsions do efficiently deliver the encapsulated drugs in the cells. However, the qualitative analysis performed here did not differentiate the uptake of non-PEG modified nanoemulsions and PEG-modified nanoemulsions.

3.3. P-gp Downregulation and Inhibition of NFκB by Curcumin. The cytosolic proteins were extracted from the CUR (20 μM) treated and untreated (control) SKOV3 and $SKOV3_{TR}$ cells, and evaluated for downregulation of P-gp and inhibition of NFkB pathway using Western blotting. The bands observed for P-gp in SKOV3 and $SKOV3_{TR}$ cells are shown in Figure 3. Lanes 1, 2, 3, and 4 represents, P-gp bands in control cells, CUR solution treated cells, CUR nanoemulsions treated cells and CUR PEG-modified nanoemulsions treated cells, respectively. Reduced band intensities were observed following the treatment with CUR suggesting that downregulation of P-gp in CUR treated SKOV3 and $SKOV3_{TR}$ cells. However, band in lane 3 was remarkably less intense compared to that of lane 2 and 4 indicating that nanoemulsion was much more efficient in downregulating the P-gp in tumor cells.

Additionally, CUR also displayed its activity against NFκB pathway. NFκB is transcription factor present in the cytoplasm as an inactive heterotrimer consisting of p50, p65 and IκBα subunits. We used anti-NFκB p65 antibody and anti-IκBα antibody to determine the inhibition of NFκB pathway. Most abundantly occurring NFκB dimers in cytoplasm contain p65 domain. The high intense NFκB bands at 64

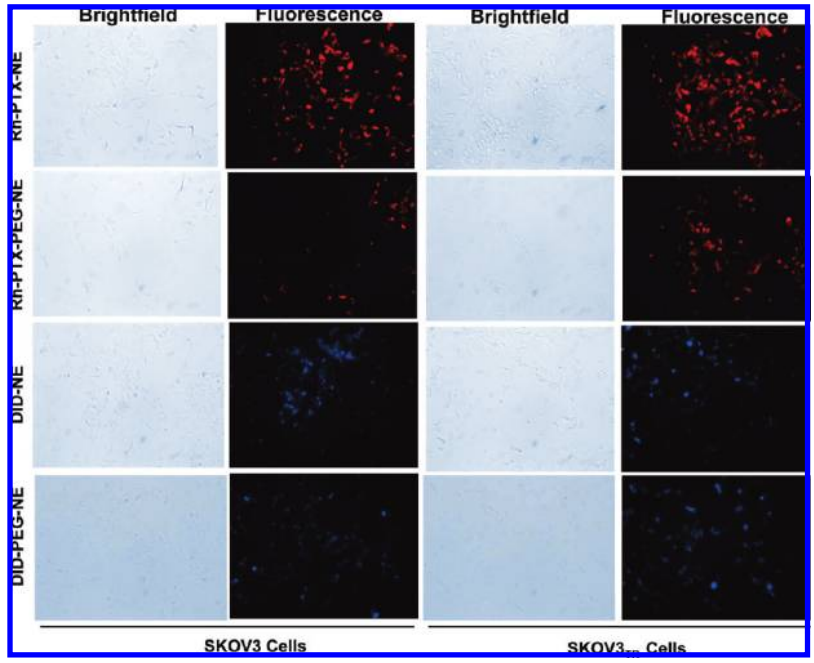

Figure 2. Brightfield and fluorescent microscopy images of rhodamine-labeled paclitaxel and DiD encapsulated nanoemulsions internalized in wild-type SKOV3 and drug resistant $SKOV3_{TR}$ human ovarian adenocarcinoma cells.

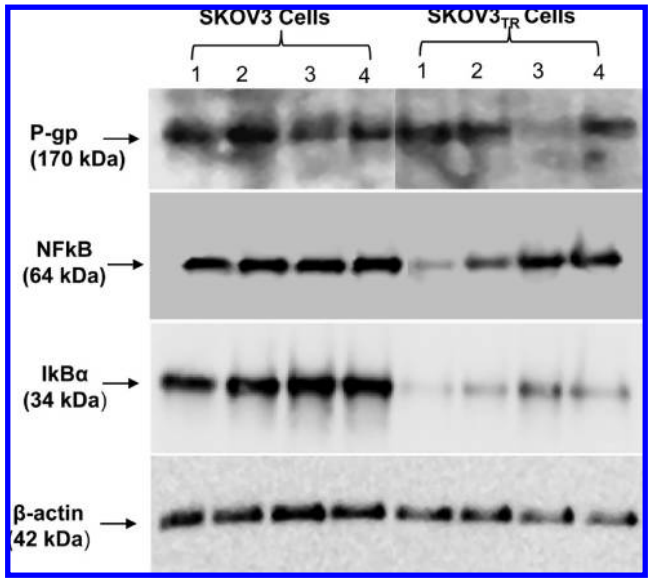

Figure 3. Western blot analysis of P-glycoprotein down-regulation and inhibition of NFκB pathway (inhibition of NFκB and IkBα) in wild-type SKOV3 and drug resistant $SKOV3_{TR}$ human ovarian adenocarcinoma cells following treatment with curcumin (20 μM). Lanes 1, 2, 3, and 4 represent untreated control, curcumin aqueous solution treated, curcumin nanoemulsion treated and curcumin PEG-modified nanoemulsion treated SKOV3 and $SKOV3_{TR}$ cells, respectively. A total of 40 and 20 μg of protein extracts were loaded per well for SKOV3 and $SKOV3_{TR}$ cells, respectively. β-Actin served as an internal loading control.

kDa were observed in CUR treated SKOV3 and $SKOV3_{TR}$ cells when compared to that of untreated cells as shown in Figure 3. This result confirmed the presence of more NFκB in cytosol in an inactive state in CUR treated cells. In untreated cells, NFκB gets translocated into the nucleus and hence less intense bands were observed. The other antibody chosen for this study was against IκBα and the band for IκBα observed at 34 kDa. Similar to NFκB, high intense bands of IκBα from CUR treated cells confirm the presence of more IκBα in cytosol and the inhibition of the NFκB pathway. CUR nanoemulsions further intensified the NFκB and IκBα bands compared to other treatments suggesting that nanoemulsions were efficient in delivering the CUR to the tumor cells. β-Actin bands with the same intensity in all the lanes served as a loading control in this study.

3.4. Cytotoxicity Studies in Sensitive and Resistant Cells. The dose−response studies against PTX and CUR as a single agent and in combination on sensitive and resistant cells are summarized in Table 2. The PTX solution IC_{50} for the SKOV3 cells was 9.5 nM, where as the IC_{50} for the $SKOV3_{TR}$ cells 2.9 μM. This revealed that $SKOV3_{TR}$ cells were needed at least ~300-fold higher concentration of PTX solution to achieve IC_{50} compared to its counterpart drug sensitive SKOV3 cells. $SKOV3_{TR}$ cells overexpress the classic MDR marker P-gp, in contrast to the drug-sensitive SKOV3 cells. PTX is a known substrate for the P-gp,[4] and the high dose required to achieve cytotoxicity was attributed to P-gp transporter mediated drug efflux in $SKOV3_{TR}$ cells. Nanoemulsion was highly efficient in delivering the PTX to both SKOV3 and $SKOV3_{TR}$ cells. A 1.8-fold reduction in concentration was noted when the PTX administered in nanoemulsion compared to PTX solution in SKOV3 cells. Similarly, the PTX delivered in nanoemulsions to $SKOV3_{TR}$ cells showed a 1.2-fold lowered concentration. However, the

Table 2. The 50% Inhibitory Concentration Values of Paclitaxel and Curcumin Alone and in Combination on SKOV3 and $SKOV3_{TR}$ Cells, Administered in the Form of Solution, Nanoemulsion and PEG-Modified Nanoemulsion[a]

	IC_{50} values	
treatment type	on SKOV3 cells	on $SKOV3_{TR}$ cells
paclitaxel solution	9.5 ± 1.2 nM	2.9 ± 0.4 μM
paclitaxel nanoemulsion	5.2 ± 1.3 nM	2.3 ± 0.1 μM
paclitaxel PEG-modified nanoemulsion	10.4 ± 0.8 nM	2.6 ± 0.3 μM
curcumin solution	9.8 ± 0.2 μM	10.8 ± 1.3 μM
curcumin nanoemulsion	6.2 ± 1.2 μM	9.6 ± 0.6 μM
curcumin PEG-modified nanoemulsion	9.4 ± 0.1 μM	10.6 ± 0.2 μM
paclitaxel + curcumin solution	4.1 nM + 5 μM	1.6 μM + 5 μM
paclitaxel + curcumin nanoemulsion	0.7 nM + 5 μM	1.1 + 5 μM
paclitaxel + curcumin PEG-modified nanoemulsion	4.5 nM + 5 μM	1.5 + 5 μM

[a] The values are shown as mean ± SD, $n = 8$.

Table 3. Paclitaxel and Curcumin Combination Index (CI) against SKOV3 and $SKOV3_{TR}$ Cells[a]

	SKOV3 cells		$SKOV3_{TR}$ cells	
combination type	CI	interaction type	CI	interaction type
paclitaxel + curcumin solution	0.94	synergistic	1.0	additive
paclitaxel + curcumin nanoemulsion	0.93	synergistic	1.0	additive
paclitaxel + curcumin PEG-modified nanoemulsion	1.0	additive	1.0	additive

[a] CI < 1, synergistic; CI = 1, additive; CI > 1, antagonistic.

PEG-modified nanoemulsion was not as effective as plain nanoemulsion. We speculate that the hydrophilic PEG chains were forming as a steric barrier and reducing the nanoemulsion uptake by the tumor cells. As seen from Table 2, CUR also exhibited anticancer activity. However, the dose−response against CUR was nearly identical in both drug-sensitive and resistant cells. CUR containing nanoemulsion showed enhanced cytotoxicity compared to CUR solution ($p < 0.05$) and PEG-modified nanoemulsion ($p < 0.05$).

To inhibit the P-gp and sensitize the $SKOV3_{TR}$ cells to PTX, we carried out the combination study and results are presented in Table 3. CUR inhibits the function of three major ABC drug transporters (P-gp, MRP-1 and ABCG2).[16,17] Therefore, the coadministration of CUR could sensitize P-gp overexpressing cells to PTX. The results revealed that, in the presence of CUR solution, the IC_{50} of PTX solution was reduced to ∼1.8-fold in $SKOV3_{TR}$ cells and 2.3-fold in SKOV3 cells. This combination therapy was significantly effective ($P < 0.05$) when the PTX and CUR delivered in nanoemulsion formulations compared to solution or in PEG-modified nanoemulsion. Overall, the use of PTX and CUR together resulted in enhanced therapeutic potential. The drugs coadministered either in solution or nanoemulsion produced synergistic cytotoxicity effect in drug-sensitive cells, whereas the drugs coadministered in solution, nanoemulsion or PEG-modified nanoemulsions produced additive cytotoxicity effect in $SKOV3_{TR}$ cells.

3.5. Quantitative and Qualitative Cellular Apoptotic Activity. To further confirm that the therapeutic potential of combination therapy was due to enhancement in cellular apoptotic activity, quantitative and qualitative apoptotic analysis was performed. Figure 4 shows the relative caspase-3/7 activities upon treatment with single and combination PTX and CUR in aqueous solution and in nanoemulsion formulations. The caspase-3/7 activities were calculated relative to the activity in untreated cells. PTX and CUR delivered in nanoemulsions induced significantly ($p < 0.05$) greater caspase-3/7 activity compared to aqueous solution and PEG-modified nanoemulsion. Additionally, as compared with PTX and CUR in aqueous solution, nanoemulsion mediated delivery of combination therapy significantly ($p < 0.05$) enhanced caspase-3/7 activities in SKOV3 and $SKOV3_{TR}$ cells. These results collaborate with the cell viability data to confirm that nanoemulsions were effective in delivering the payload to the cells, and combination therapy with PTX and CUR delivered in nanoemulsions produced potential therapeutic effects.

The results in Figure 5 show quantitative apoptotic activity in SKOV3 and $SKOV3_{TR}$ cells by Vybrant Apoptosis assay using flow cytometry following the treatment of cells for 24 h. In this assay, the YO-PRO-1 (green, apoptotic cell permeant) dye and propidium iodide (red, apoptotic cell impermeant) were used to label and differentiate between the live cells, those undergoing apoptosis, and those that were dead. The flow cytometry plots reveal that there was enhancement in cellular apoptosis in both SKOV3 and $SKOV3_{TR}$ cells when PTX and CUR were administered in nanoemulsion formulations as compared to aqueous solutions ($p < 0.05$). In addition, when PTX and CUR were coadministered in nanoemulsions, there was an increase in apoptosis at lower doses (i.e., 42.6% apoptosis in SKOV3 with 5 nM PTX and 5 μM CUR, 18.3% apoptosis in $SKOV3_{TR}$ cells with 2 μM PTX and 5 μM CUR).

Additionally, qualitative analysis of cellular apoptosis after single and combination therapy was evaluated using TUNEL assay. It determines apoptosis as a result of DNA fragmentation occurring in the apoptotic cells due to drug treatment. The apoptotic nuclei are stained brown by a three-step

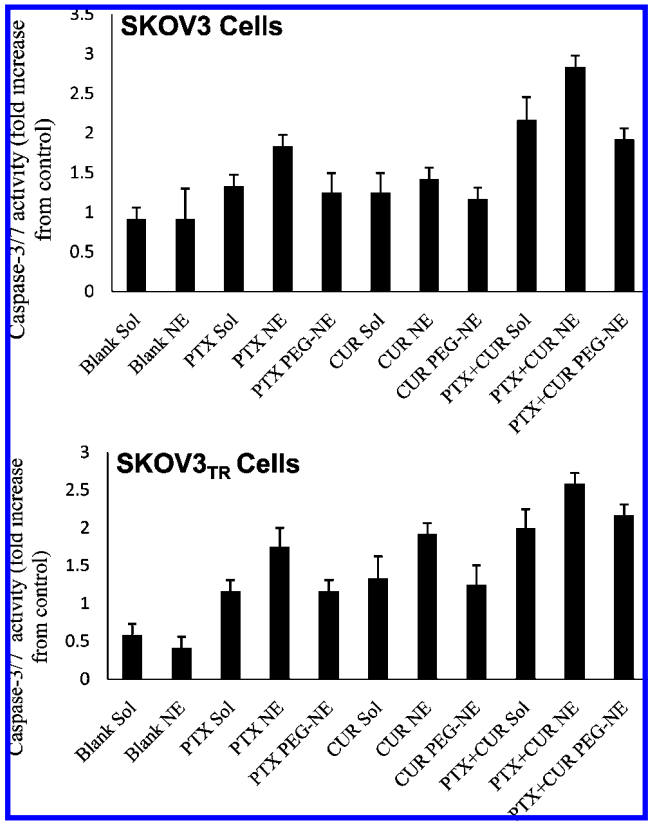

Figure 4. Caspase-3/7 activation, as measured by relative increase to baseline, in SKOV3 and $SKOV3_{TR}$ cells following treatment with paclitaxel and curcumin either as a single agent or in combination, when administered in aqueous solution, nanoemulsion, and PEG-modified nanoemulsion formulations. The results represent mean ± SD ($n = 4$). Statistically significant when caspase-3/7 activity of paclitaxel nanoemulsion (PTX NE) is compared with paclitaxel solution (PTX Sol) and curcumin nanoemulsion (CUR NE) is compared with curcumin solution (CUR Sol) in both cell types at $p < 0.05$. Similarly, the coadministration of paclitaxel and curcumin in nanoemulsions (PTX+CUR NE) showed statistically significant activity compared to solution form at $p < 0.05$.

mechanism that involves incorporation of biotinylated nucleotides at 3′-OH DNA end, binding of horseradish peroxidase-labeled streptavidin to the incorporated nucleotides, and finally the detection of the nucleotides with the help of peroxidase substrate, diaminobenzidine, which results in the formation of the dark brown stains. As shown in Figure 6, the positively stained cells seemed to have dark brown nuclei. The untreated cells did not show brown color nuclei suggesting no apoptosis in these cells. However, the cells treated with PTX and CUR in solution and nanoemulsions formulations showed characteristics dark brown staining of the nuclei that is representative of apoptotic cells. Combination PTX and CUR therapy resulted in the highest degree of apoptosis and led to the most pronounced dark brown staining.

4. Discussion

Nanoemulsions are thermodynamically stabilized dispersions of oil in water, where the oil droplet size is reduced to nanometer length scale (<200) by applying high shear stress using high energy ultrasonication or microfluidizing instruments.[19,25,27] They have been successfully investigated as carriers for delivery of liphophilic anticancer drugs.[18,19,25,28] When liphophilic compounds are incorporated into the nanoemulsions, the pharmacokinetic and biodistribution pattern of the compounds upon systemic administration will be dictated by the properties of the nanoemulsions formulations rather the physicochemical characteristics of the drug molecules. For example, the PEG-modification can enhance the longevity of the nanoemulsions in the blood circulation. This in turn increases the residence time of the drug molecules in the blood and also allows enhanced accumulation at the tumor site through the EPR effect.[29] Additionally, nanoemulsions can be attached with target-specific ligands for site-specific localization.[27] Based on this fact, a variety of different anticancer therapies can be incorporated into the nanoemulsion systems for target-specific systemic delivery to the tumor site.

In this study, we have developed an optimized oil-in-water nanoemulsion formulation using flaxseed oil, which has a high concentration of PUFA. Egg lecithin was incorporated to allow for stabilization of the nanoemulsions due to adsorption of this agent at the oil−water interface and lowering of the interfacial tension. It is important to note that there are few individuals who are allergic to egg lecithin.[30] In general, all the nanoemulsions showed oil droplet size below 150 nm with narrow size distribution (Table 1). TEM image in Figure 1 also confirms that the oil droplets were spherical and uniformly distributed. PEG surface modification of nanoemulsions using $DSPE\text{-}PEG_{2000}$ did not affect the particle size and size distribution. The surface charge values of the nanoemulsions were observed in the range of −35.37 to −44.53 mV. The surface charge on the nanoemulsion oil droplets is representative of the ionization of the components forming the interfacial layer. In nanoemulsions, the interfacial layer is formed by adsorption of egg lecithin. In case of PEG-modified nanoemulsions, the interfacial layer was formed as a result of egg lecithin and PEG-modified phospholipid ($DSPE\text{-}PEG_{2000}$). These formulations were used to deliver PTX and CUR for combination therapy against SKOV3 and $SKOV3_{TR}$ cells. The qualitative cellular uptake analysis demonstrated that the nanoemulsion formulations were efficiently internalized

(27) Sarker, D. K. Engineering of nanoemulsions for drug delivery. *Curr. Drug Delivery* **2005**, *2*, 297–310.
(28) Patlolla, R. R.; Vobalaboina, V. Pharmacokinetics and tissue distribution of etoposide delivered in parenteral emulsion. *J. Pharm. Sci.* **2005**, *94* (2), 437–445.
(29) Maeda, H.; Wu, J.; Sawa, T.; Matsumura, Y.; Hori, K. Tumor vascular permeability and the EPR effect in macromolecular therapeutics: a review. *J. Controlled Release* **2000**, *65* (1−2), 271–284.

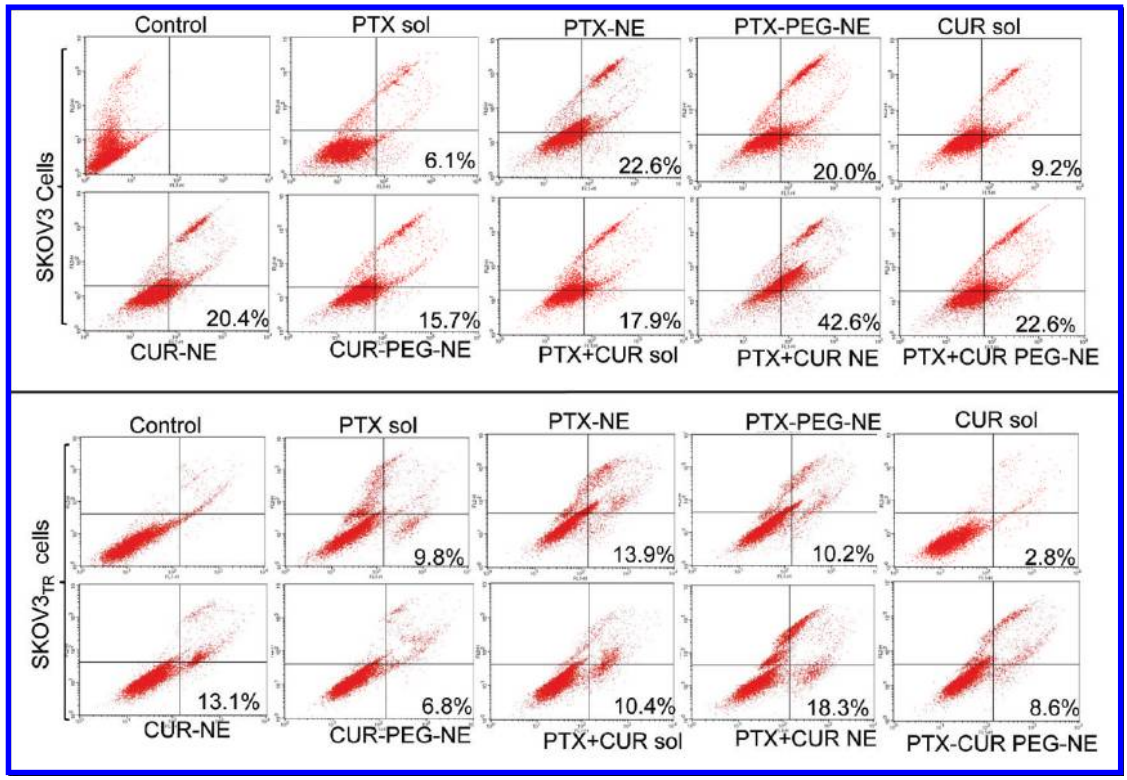

Figure 5. Flow cytometry analysis of quantitative apoptotic activity measurements in wild-type SKOV3 and drug resistant $SKOV3_{TR}$ human ovarian adenocarcinoma cells after the treatment with paclitaxel and curcumin either as a single agent or in combination, when administered in aqueous solution, nanoemulsion and PEG-modified nanoemulsion. Flow cytometry was performed following 24 h of treatment. Statistically significant when apoptotic activity of paclitaxel nanoemulsion (PTX NE) and PEG-modified nanoemulsion (PTX PEG-NE) is compared with paclitaxel solution (PTX Sol) and curcumin nanoemulsion (CUR NE) is compared with curcumin solution (CUR Sol) in both cell types at $p < 0.05$. The apoptosis was significantly greater with the combination therapy and with drugs administered in nanoemulsions at $p < 0.05$.

in SKOV3 and $SKOV3_{TR}$ cells (Figure 2). This suggests that the nanoemulsions do efficiently deliver the payload to the subcellular sites in the cell.

Overexpression of P-gp, especially in tumor cells, will not allow drugs to accumulate in the cells and results in reduced cytotoxicity. Combination of P-gp inhibitors and conventional chemotherapeutic drugs was found to be efficacious in treating tumors.[31,32] CUR was found to inhibit P-gp overexpression and can reverse the MDR phenomenon.[16,17] It was also found that P-gp does not confer resistance to CUR and also modulation of P-gp by CUR was not cell type dependent.[33] In this study, we found that CUR downregulates P-gp in $SKOV3_{TR}$ cells and SKOV3 cells (Figure 3). The more pronounced downregulation of P-gp was observed when the CUR was delivered in nanoemulsion formulations. Based on this evidence, we propose that CUR can prevent PTX drug resistance mediated by P-gp transporter and, in addition, can also improve the systemic availability of the PTX that have limited intestinal absorption due to active efflux by P-gp transporter. In addition to P-gp downregulation, CUR blocks the classical NFκB pathway which regulates inflammation, cell proliferation and apoptosis in normal cells.[15] NFκB pathway controls the expression of genes involved in the antiapoptotic processes, and this is responsible for tumor cell survival and metastasis.[13] NFκB is a transcription factor present in the cytoplasm as an inactive heterotrimer consisting of p50, p65 and IκBα subunits. In response to specific stimuli, IκB kinase (IKK) phosphorylates and degrades IκBα subunit, thus NFκB translocates into the nucleus and initiates the transcription of several genes responsible for tumor cell survival and

(30) Hofer, K. N.; McCarthy, M. W.; Buck, M. L.; Hendrick, A. E. Possible anaphylaxis after propofol in a child with food allergy. *Ann. Pharmacother.* **2003**, *37* (3), 398–401.

(31) Meerum Terwogt, J. M.; Malingre, M. M.; Beijnen, J. H.; ten Bokkel Huinink, W. W.; Rosing, H.; Koopman, F. J.; van Tellingen, O.; Swart, M.; Schellens, J. H. M. Coadministration of oral cyclosporin A enables oral therapy with paclitaxel. *Clin. Cancer Res.* **1999**, *5* (11), 3379–3384.

(32) Britten, C. D.; Baker, S. D.; Denis, L. J.; Johnson, T.; Drengler, R.; Siu, L. L.; Duchin, K.; Kuhn, J.; Rowinsky, E. K. Oral paclitaxel and concurrent cyclosporin A: targeting clinically relevant systemic exposure to paclitaxel. *Clin. Cancer Res.* **2000**, *6* (9), 3459–3468.

(33) Chearwae, W.; Anuchapreeda, S.; Nandigama, K.; Ambudkar, S. V.; Limtrakul, P. Biochemical mechanism of modulation of human P-glycoprotein (ABCB1) by curcumin I, II, and III purified from Turmeric powder. *Biochem. Pharmacol.* **2004**, *68* (10), 2043–2052.

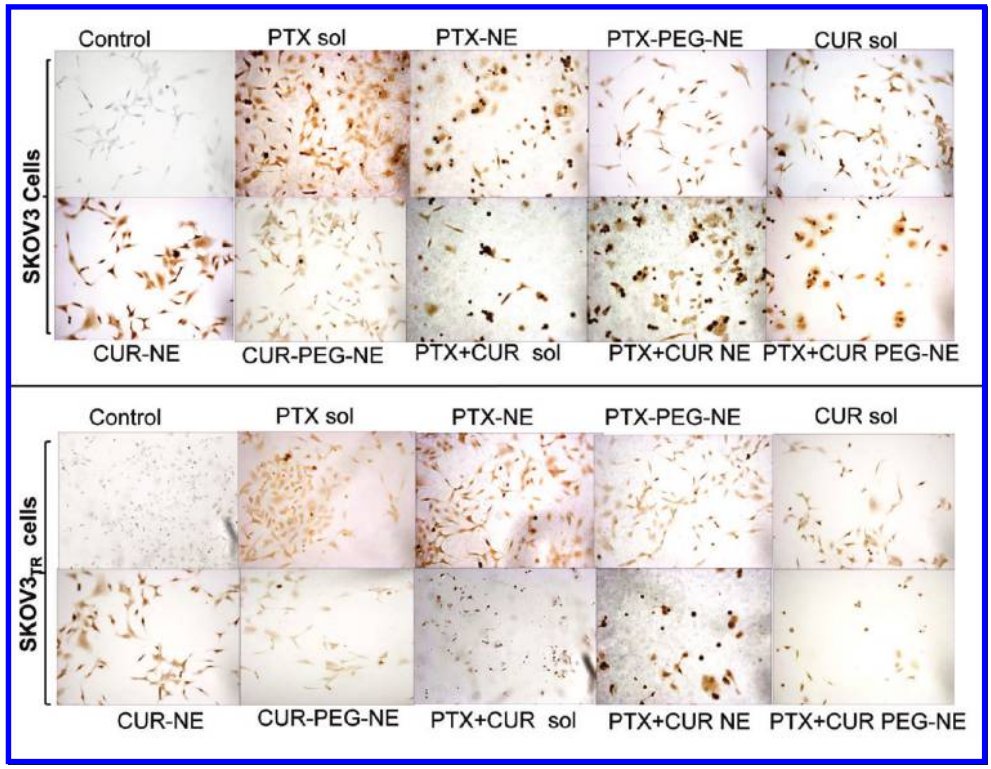

Figure 6. Qualitative analysis of cellular apoptosis in wild-type SKOV3 and drug resistant $SKOV3_{TR}$ human ovarian adenocarcinoma cells using TUNEL staining upon treatment with paclitaxel and curcumin, either alone or in combination in aqueous solution, nanoemulsion, and PEG-modified nanoemulsion formulations for 24 h. Original magnification was 20×.

metastasis.[13,14] CUR inhibits IKK and thus inhibits the degradation of IκBα. NFκB remains in the inactive state as long as IκBα is not degraded. This results in enhanced apoptosis in tumor cells. This Western blot analysis (Figure 3) confirmed that NFκB pathway was blocked by CUR in SKOV3 and $SKOV3_{TR}$ cells. Overall, the P-gp downregulation and inhibition of NFκB pathway by CUR could augment the anticancer activity of PTX against SKOV3 and $SKOV3_{TR}$ cells. In addition, these results also suggest that CUR has a role in prevention or treatment of human ovarian cancer.

We have examined the effect of PTX and CUR combination therapy on proliferation of SKOV3 and $SKOV3_{TR}$ cells (Table 2 and Table 3). The combination therapy significantly suppressed the growth of both cell types even at lower doses. The cytotoxicity effects were even more pronounced when the drugs administered in nanoemulsion formulation. The enhanced therapeutic activity observed with the combination therapy was attributed to the P-gp downregulation and inhibition of NFκB pathway by CUR. P-gp downregulation helps by increasing the accumulation of PTX within the tumor cell and overcoming the MDR phenomenon.[17] Inhibition of NFκB pathway could contribute to enhanced apoptosis process in tumor cells.[15]

Quantitative apoptotic activity measurements were made by evaluating caspase-3/7 activity and flow cytometry analysis in PTX and CUR treated cells. The enhanced caspase-3/7 activity was noted following the treatment with PTX and CUR as single agents or in combination. This suggests that both PTX and CUR induce apoptosis in tumor cells. The PTX and CUR combination therapy was even more efficient in inducing the apoptosis in both cell lines used in the study. Nanoemulsions also seemed to play a role in enhanced activity by effective internalization of the drugs. As compared with PTX and CUR in aqueous solution, nanoemulsion mediated delivery of PTX and CUR significantly enhanced caspase-3/7 activities in SKOV3 and $SKOV3_{TR}$ cells (Figure 4). In addition to these observations, flow cytometry analysis also revealed that the combination therapy was highly effective in inducing the cellular apoptosis and cell death (Figure 5). The characteristic dark brown staining of the nuclei by TUNEL staining indicated that the treated cells underwent apoptosis (Figure 6). Again, the combination therapy resulted in the highest degree of apoptosis and led to the most pronounced dark brown staining. These results collaborate with the cell viability data to confirm that nanoemulsions were effective in delivering the PTX and CUR to the cells, and combination therapy with PTX and CUR delivered in nanoemulsions indeed showed higher therapeutic efficacy in SKOV3 and $SKOV3_{TR}$ cells. All these results indicate that CUR could potentiate the apoptotic effects of PTX against SKOV3 and $SKOV3_{TR}$ cells.

5. Conclusions

When cancer cells develop a MDR phenotype either due to intrinsic factors, such as microenvironmental selection pressures, or after first exposure to a chemotherapeutic agent, the ensuing clinical outcomes are always very poor. Strategies that allow for enhancement of systemic delivery efficiency as well as augmentation of therapeutic response by lowering tumor apoptotic threshold can have a profound impact in the management of refractory diseases. In this study, we have examined coadministration of PTX and CUR using nanoemulsion formulations that can aid in enhancing delivery efficiency to the tumor mass. The oil-in-water nanoemulsion can also solubilize hydrophobic compounds, such as PTX and CUR, and allow for efficient intracellular delivery. The pleiotropic effects of CUR are especially beneficial in refractory cancer due to inhibition of NFκB activity and downregulation of important efflux transporters such as P-gp, and MRP-1 in tumor cells. Combination PTX and CUR when administered in nanoemulsion formulations showed significant enhancement in cytotoxicity, especially in drug resistant $SKOV3_{TR}$ ovarian adenocarcinoma cells. This dual therapeutic strategy can have significant potential in the clinical management of refractory diseases. Future *in vivo* studies in human tumor xenograft models will further validate this hypothesis.

Acknowledgment. This study was supported by the National Cancer Institute's Alliance in Nanotechnology for Cancer Platform Partnership grant (R01-CA119617). Transmission electron microscopy was performed by Mr. William Fowle at the Electron Microscopy Center of Northeastern University. Additionally, the authors are deeply grateful to Dr. Robert Campbell for assistance with the particle size analysis.

MP800240J